Lensing and Photon Rings in a Magnetized Black Hole Environment

Muhammad Haider Khan*
Erasmus Mundus Joint Master (EMJM) Master in Astrophysics and Space Science.
(Dated: July 31, 2025)

We analyse null geodesics and photon rings in the Schwarzschild–Melvin (Ernst) spacetime. In the equatorial plane ($\theta = \pi/2$) for subcritical fields $B < B_c$, circular photon orbits satisfy a cubic equation, yielding an inner unstable orbit and an outer stable orbit that coalesce at $B = B_c$. Restricting to constant–ϕ (meridional) slices, conformal equivalence to Schwarzschild guarantees an unstable photon orbit at $r = 3M$, and we prove that no spherical lightlike geodesics exist for $B \neq 0$. We derive the exact meridional light-deflection integral, divergent as the periastron approaches $3M$, and obtain closed-form expressions for the shadow's vertical (α) and horizontal (β) angular radii, showing that α remains Schwarzschild–identical while β is enhanced by B, so that $\beta > \alpha$. Finally, applying the strong-deflection formalism to each meridional slice, we compute the critical value of $(L/E)_n$ for the photon rings and the gap parameter Δ_n, and identify how the outermost stable circular orbit bounds the emitter radius.

I. INTRODUCTION

Gravitational lensing and shadow formation by black holes depend fundamentally on the behaviour of null geodesics. We investigate such geodesics in the Schwarzschild-Melvin (Ernst) spacetime, which describes a Schwarzschild black hole of mass M immersed in a uniform magnetic field of strength B [1]. The magnetic field enters the metric via a factor $\Lambda(r, \theta, B)$. While real astrophysical fields are not perfectly uniform, the Ernst solution provides an analytically tractable model for studying the interplay of gravity and magnetism in strong-field lensing.

In the equatorial plane ($\theta = \pi/2$), null circular orbits satisfy a cubic equation. Dhurandhar and Sharma [2] and Esteban [3] showed that for subcritical fields $B < B_c$ this equation has two real positive roots outside the horizon: an inner unstable photon orbit r_2 (deforming continuously from $r = 3M$) and an outer stable photon orbit r_1. At the critical field B_c these two roots merge, and for $B \geq B_c$ no circular photon orbit exists outside $r = 2M$. Crucially, Junior *et al.* [4] showed that each constant-ϕ (meridional plane) slice of Ernst spacetime is conformal to the Schwarzschild geometry. Hence null geodesics in a meridional plane follow the same spatial paths as in Schwarzschild, up to a reparametrization. In particular, each meridional plane contains an unstable photon orbit at $r = 3M$, forming a two-dimensional fundamental photon orbit surface. Therefore, the familiar photon sphere physics of Schwarzschild applies in each meridional slice. Spherical geodesics refer to the geodesics that stay at a particular radius value while oscillating in the θ direction. We analytically prove that spherical lightlike geodesics are not possible in the Ernst spacetime.

We derive closed-form expressions for the shadow's angular radius in both vertical (meridional) and horizontal (equatorial) directions. Photon rings, an infinite sequence of highly lensed images from photons orbiting near the photon sphere, are governed by these unstable orbits. Extending this concept to the magnetized case is the focus of our work, and we apply the strong-deflection lensing formalism to compute the sequence of photon rings for an observer at a finite distance.

This paper is organized as follows: In Sec. II, we review the Ernst metric. In Sec. III, we analyse lightlike and timelike geodesics in the Ernst spacetime. Sec. IV includes the angular deflection expressions for the meridional and equatorial planes. In Sec. V, we derive angular shadow radii. Sec. VI introduces the photon ring formalism and presents our results on the photon ring sequence. We conclude with Sec. VII.

II. SPACETIME

The Schwarzschild-Melvin (Ernst) metric is a static, axisymmetric solution of the Einstein-Maxwell equations for a Schwarzschild black hole of mass M immersed in an external uniform magnetic field B. In Schwarzschild coordinates (t, r, θ, φ) it reads

$$ds^2 = -\Lambda^2 \left(1 - \frac{2M}{r}\right) dt^2 + \frac{\Lambda^2}{\left(1 - \frac{2M}{r}\right)} dr^2 + r^2 \Lambda^2 d\theta^2 + \frac{r^2 \sin^2\theta}{\Lambda^2} d\phi^2 \quad (1)$$

where the factor Λ is defined as,

$$\Lambda = 1 + \frac{1}{4} r^2 B^2 \sin^2\theta. \quad (2)$$

The event horizon remains at $r = 2M$, as in Schwarzschild. However, unlike Schwarzschild, this spacetime is not asymptotically flat: at large r the metric approaches the Melvin-Bonnor magnetic universe [5, 6]. In the limit $B \to 0$, we recover the Schwarzschild metric.

* haider4251@gmail.com

III. GEODESICS IN THE ERNST SPACETIME

The following Lagrangian governs the geodesics in the Ernst spacetime

$$\mathcal{L} = \frac{1}{2}\Bigg[-\frac{1}{\Lambda^2(1-\frac{2M}{r})}E^2 + \frac{\Lambda^2}{r^2\sin^2\theta}L^2 + \frac{\Lambda^2}{(1-\frac{2M}{r})}\dot{r}^2 + r^2\Lambda^2\dot{\theta}^2\Bigg] = \frac{1}{2}\epsilon \tag{3}$$

where E and L are the conserved quantities corresponding to the time-translation and axial symmetries, respectively

$$\frac{\partial\mathcal{L}}{\partial\dot{t}} = -E = \Lambda^2\left(1-\frac{2M}{r}\right)\dot{t}, \tag{4}$$

$$\frac{\partial\mathcal{L}}{\partial\dot{\phi}} = L = \frac{r^2\sin^2\theta}{\Lambda^2}\dot{\phi}. \tag{5}$$

The constant ϵ has values of 0 and -1 for lightlike and timelike particles, respectively.

A. Circular Lightlike Geodesics

Circular lightlike orbits require

$$\epsilon = 0,$$
$$\dot{r} = \ddot{r} = 0,$$
$$\dot{\phi} = \ddot{\phi} = 0.$$

Applying these conditions, we find that they hold only in the equatorial plane ($\theta = \pi/2$), leading to the cubic equation

$$3B^2r^3 - 5MB^2r^2 - 4r + 12M = 0. \tag{6}$$

Dhurandhar and Sharma [2] and Esteban [3] showed that for magnetic field strength B values below a critical value,

$$B_c = \frac{0.189366386}{M} \tag{7}$$

the cubic equation (6) admits up to three real roots. There exist two physical roots r_1 and r_2 (where $r_2 < r_1$) outside the event horizon. The third root r_3 remains unphysical for all B as it lies within the horizon. See Appendix A for the closed-form expressions of these solutions. Dhurandar and Sharma [2] define an effective potential for light rays in the equatorial plane

$$V_{eff} = \frac{\Lambda^4}{r^2}\left(1-\frac{2M}{r}\right) \tag{8}$$

which satisfies the orbital equation

$$\left(\frac{dr}{d\phi}\right)^2 = \frac{r^4}{\Lambda^8}\left(\frac{E^2}{L^2} - V_{eff}\right). \tag{9}$$

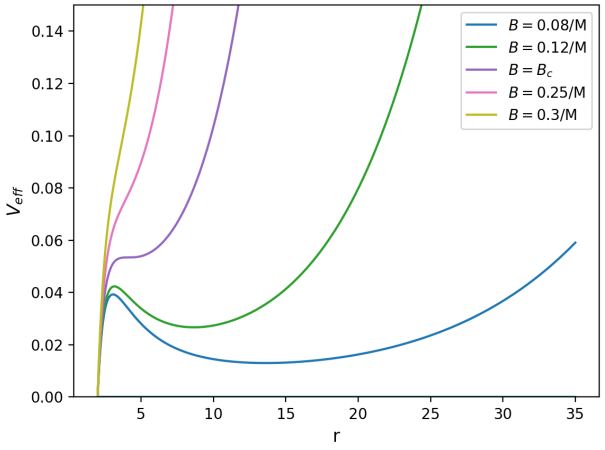

FIG. 1. Equatorial effective potential V_{eff}.

V_{eff} is plotted in Fig. (1) for various B values. The maximum and the minimum of the plots correspond, respectively, to the unstable (r_2) and stable (r_1) circular lightlike geodesics in the equatorial plane. At $B = B_c$ these roots coincide and disappear. For $B > B_c$ no critical points exist and hence we do not have any circular lightlike geodesics.

B. Meridional Conformality and Fundamental Photon Orbits

Junior et al. [4] identified that when reduced to a meridional plane $\dot{\phi} = 0$, the Ernst spacetime is conformal to the constant-ϕ hypersurfaces of the Schwarzschild spacetime. Since null geodesics are conformally invariant, defining a new affine parameter $\tilde{\lambda}$ such that

$$\Lambda\frac{d}{d\lambda} \to \frac{d}{d\tilde{\lambda}},$$

which recasts the equations of motion into Schwarzschild form. Hence, the Lagrangian takes the form:

$$\mathcal{L} = \frac{1}{2}\Bigg[-\left(1-\frac{2M}{r}\right)\dot{\tilde{t}}^2 + \frac{1}{\left(1-\frac{2M}{r}\right)}\dot{\tilde{r}}^2 + r^2\dot{\tilde{\theta}}^2\Bigg].$$

The conserved quantities are now,

$$\frac{\partial\mathcal{L}}{\partial\dot{\tilde{t}}} = -E = \left(1-\frac{2M}{r}\right)\dot{\tilde{t}}, \tag{10}$$

$$\frac{\partial\mathcal{L}}{\partial\dot{\tilde{\theta}}} = \tilde{L} = r^2\dot{\tilde{\theta}}. \tag{11}$$

Here $\tilde{L}$ is the angular momentum arising from the cylicity of the θ coordinate in the meridional plane of the

Ernst spacetime. Now, we have 3 conserved quantities: $E, \tilde{L}$ and $\mathcal{L}$ and a $(2+1)$-dimensional system in the meridional plane, making the geodesic equations fully integrable.
Together, the null geodesics sweep out a 2-dimensional surface at $r = 3M$ termed as *Fundamental Photon Orbits* by Junior et al. [4].

$$ds^2|_{t=cte.,r=3M} = (3M)^2 \left[\Lambda^2 d\theta^2 + \frac{\sin^2\theta}{\Lambda^2} d\phi^2\right]. \quad (12)$$

However, it must be identified that these orbits going through the poles are not circular, unlike the lightlike orbits in the equatorial plane as described in Sec. III A. The intrinsic geometry of the spacetime leads to an elongated trajectory resulting in non-circular orbits.

C. Spherical Lightlike Geodesics

Geodesics that stay at a constant radius value while oscillating in the θ direction are called spherical geodesics. We prove analytically that the Ernst spacetime does not admit spherical lightlike geodesics. Spherical geodesics require the condition

$$\dot{r} = 0, \quad \ddot{r} = 0. \quad (13)$$

Using these and $\epsilon = 0$ in the Lagrangian (3), we get the following condition on the geodesic constants

$$\frac{L^2}{E^2} = \frac{r(r-3M)}{\Lambda^3 B^2 (r-2M)^2}. \quad (14)$$

Note that this equation holds true when $r = 3M$ leading to $L = 0$ which is the case of the fundamental photon orbit as discussed in Sec. III B. Except for the meridional plane, since L and E are constants, it demands Λ to be a constant as well, meaning that if

$$B \neq 0 \implies \dot{\theta} = 0 \quad (15)$$

Hence, for a non-zero magnetic field strength, we cannot have spherical lightlike orbits.

D. Circular Timelike Geodesics

For massive (timelike) uncharged particles we set $\epsilon = -1$ in Eq. (3) yielding

$$-\frac{1}{\Lambda^2(1-\frac{2M}{r})}E^2 + \frac{\Lambda^2}{r^2\sin^2\theta}L^2 + \frac{\Lambda^2}{(1-\frac{2M}{r})}\dot{r}^2 + r^2\Lambda^2\dot{\theta}^2 = -1, \quad (16)$$

For circular geodesics, we require $\dot{r} = \ddot{r} = 0$ and $\dot{\phi} = \ddot{\phi} = 0$, and we get the orbital equation

$$\frac{1}{2}\left(\frac{dr}{d\phi}\right)^2 + V_{E,L} = 0,$$

where we defined an effective potential $V_{E,L}$ given by

$$-2V_{E,L} = \frac{r^4}{L^2\Lambda^4}\left[\frac{E^2}{\Lambda^4} - \left(1-\frac{2M}{r}\right)\left(\frac{L^2}{r^2} + \frac{1}{\Lambda^2}\right)\right]. \quad (17)$$

For circular orbits, we have the conditions

$$V_{E,L} = 0, \quad V'_{E,L} = 0.$$

Figure (2) provides a plot of $V_{E,L}$ for different value of B. For circular timelike observers, we get the equations

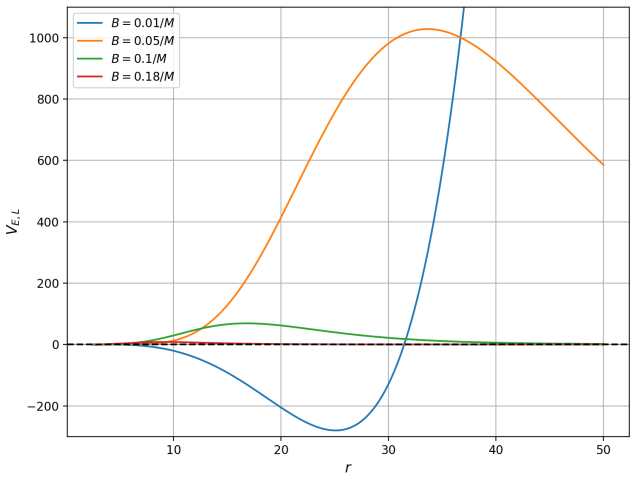

FIG. 2. Effective Potential $V_{E,L}$ for Timelike Observer for various B values.

for E^2 and L^2 in terms of r

$$E^2 = \frac{\Lambda\left(4Mr^2B^2 - 4r + 8M + \frac{1}{4}B^4r^5 + MB^4r^4\right)}{\left(1-\frac{2M}{r}\right)^{-1}\left(3B^2r^3 - 5MB^2r^2 - 4r + 12M\right)}, \quad (18)$$

$$L^2 = \frac{r^2}{\Lambda^2}\left[\frac{4Mr^2B^2 - 4r + 8M + \frac{1}{4}B^4r^5 + MB^4r^4}{\Lambda(3B^2r^3 - 5MB^2r^2 - 4r + 12M)} - 1\right]. \quad (19)$$

In Schwarzschild spacetime, circular timelike orbits exist for $r > 3M$. In Ernst spacetime, however, one finds numerically that $L^2 > 0$ only in the range

$$r_2 < r < r_1,$$

where r_1 and r_2 are the two positive roots of the cubic equation (6) indicating that circular timelike orbits can only exist between the two circular lightlike orbits in the equatorial plane. Fig (3) shows a plot of L^2 for different r values. One can show that $L^2 < 0$ for $B > B_c$ indicating that we cannot have circular timelike orbits for a supercritical magnetic field strength.
Fig 4 shows $V''_{E,L}(r)$ for various B. Each curve crosses zero exactly once at $r = r_{ISCO}$, and remains positive until $r < r_1$. Where r_{ISCO} denotes the innermost stable

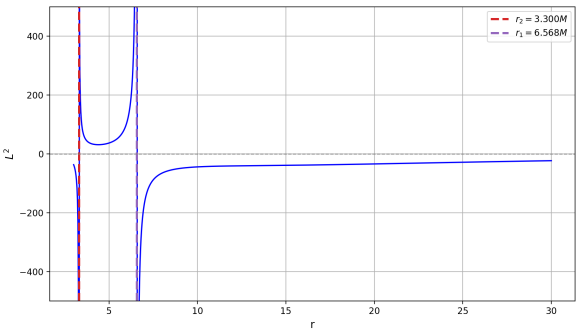

FIG. 3. L^2 plotted for a range of r for $B = 0.15/M$.

circular orbit, where $V''_{E,L} = 0$. We identify the region of stable timelike circular orbits:

$$r_{ISCO} < r < r_1 \tag{20}$$

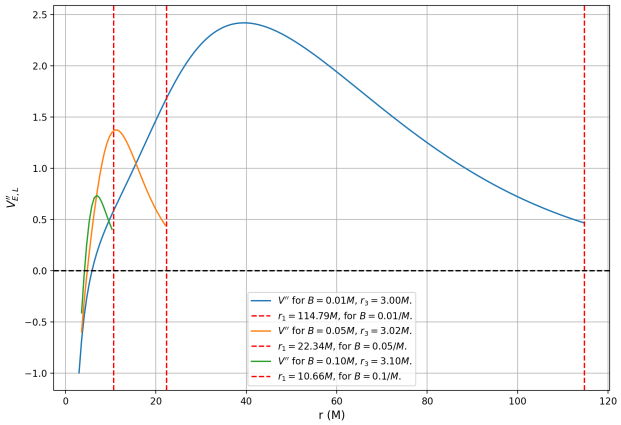

FIG. 4. $V''_{E,L}$ for various B values.

IV. ANGULAR DEFLECTION

A. Meridional Plane

In the meridional plane, the null geodesics are identical to those in Schwarzschild. The trajectory equation for the meridional plane is given by:

$$\frac{d\tilde{\phi}}{dr} = \left[\frac{r^4}{\Lambda^8}\left(\frac{E^2}{L^2} - \frac{\Lambda^4\left(1-\frac{2M}{r}\right)}{r^2}\right)\right]^{-1/2}. \tag{21}$$

For a light ray that goes through a minimum radius r_m we have,

$$\frac{E^2}{Q^2} = \frac{1}{r_m^2} - \frac{2M}{r_m^3}. \tag{22}$$

Using this expression in Eq. (21) and integrating over a light ray yields,

$$\delta_{\text{mer}} = 2\int_{r_m}^{\infty} \frac{r_m\, dr}{\sqrt{\left(1-\frac{2M}{r_m}\right) r^4 - r^2 r_m^2 + 2M r r_m^2}}. \tag{23}$$

This expression coincides exactly with the Schwarzschild result and, as in that case, the integral diverges in the limit $r_m \to 3M$.

B. Equatorial Plane

In contrast, when restricting to the equatorial plane ($\theta = \pi/2$), the Ernst metric does not conformally reduce to the Schwarzschild case, and we obtain the following trajectory equation

$$\frac{d\phi}{dr} = \left[\frac{r^4}{L^2\Lambda^4}\left\{\frac{E^2}{\Lambda^4} - \left(1-\frac{2M}{r}\right)\left(\frac{L^2}{r^2}+\frac{1}{\Lambda^2}\right)\right\}\right]^{-1/2}. \tag{24}$$

Integrating this for a light ray going through a minimum radius

$$\delta_{eqt} = 2\int_{r_m}^{\infty} \frac{r_m}{\sqrt{\frac{\Lambda^4(r_M)}{\Lambda^8}\left(1-\frac{2M}{r_m}\right) r^4 - \frac{r^2 r_m^2}{\Lambda^4} + \frac{2Mrr_m^2}{\Lambda^4}}} dr. \tag{25}$$

However, evaluating the expression under the square root reveals that it becomes negative for all $r < r_m$. Thus, any light ray in the equatorial plane with non-zero angular momentum cannot return to infinity. This generalizes Dhurandhar *et al.* [2], who proved that for $B > 0$ no particle with $L \neq 0$ can escape to spatial infinity. Consequently, in Ernst spacetime, no meaningful angular deflection exists in the equatorial plane for finite observers.

V. SHADOW ANGULAR RADII

We denote by α and β as, respectively, the vertical (meridional) angular radius and the horizontal (equatorial) angular radius of the Schwarzschild-Melvin black hole.

A. Vertical Angular Radius

The vertical shadow radius α is determined from the meridional photon sphere at $r = 3M$, giving:

$$\sin^2\alpha = \frac{27M^2(r_O - 2M)}{r_O^3}. \tag{26}$$

B. Horizontal Angular Radius

The horizontal shadow radius β comes from the unstable equatorial orbit at r_2:

$$\sin^2\beta = \frac{\Lambda^4(r_O,\pi/2)(r_O-2M)}{r_O^3}\cdot\frac{r_2^3}{\Lambda^4(r_2,\pi/2)(r_2-2M)}. \tag{27}$$

C. Geometry of the Shadow

To analyse the geometry of the shadow, we compare the vertical and horizontal angular radii

$$\frac{\Lambda^4(r_O)(r_O-2M)}{r_O^3}\cdot\frac{r_2^3}{\Lambda^4(r_2)(r_2-2M)} \gtrless \frac{27M^2(r_O-2M)}{r_O^3}.$$

For $r_O > r_2$, one has $\Lambda^4(r_O)/\Lambda^4(r_2) > 1$. Writing

$$r_2 = (3+\eta)\,M, \quad \eta \ll 1,$$

a binomial expansion gives

$$\frac{r_2^3}{r_2-2M} \approx 27M^2.$$

Hence

$$\frac{\Lambda^4(r_O)}{\Lambda^4(r_2)}\,\frac{r_2^3}{r_2-2M} > 27M^2 \implies \beta > \alpha. \tag{28}$$

This confirms that for all observers located at $r_O > r_2$ for $B \neq 0$, the shadow exhibits an oblate shape. This analytical result is consistent with the numerical findings of Junior et al. [4]. The two angular radii are plotted as a function of the observer radius r_O for two values of B in Fig. (5).

D. Light Sources and Shadow Geometry

Since the Ernst spacetime is not asymptotically flat, any photon with $L \neq 0$ falls back inwards [2]. Hence, we assume light sources at a large but finite radius r_S (instead of at infinity). The observer (at radius r_O) will then see bright regions in the sky corresponding to directions where backward-traced rays hit these sources, and dark (shadow) regions where rays either fall into the black hole or remain trapped.
For $r_S < r'_O$ trajectories with $E^2/L^2 \geq V_{eff}|_{r_2}$ will be reflected outwards (bright region) and those with $E^2/L^2 \approx V_{eff}|_{r_1}$ will be trapped in bound oscillatory orbit (dark regions). Those with $E^2/L^2 = V_{eff}|_{r_2}$ will spiral around r_2 and then plunge into the black hole and provide the horizontal shadow boundary. We plot the effective potential given by Eq. (8) for $B = 0.12/M$ in Fig. (6).

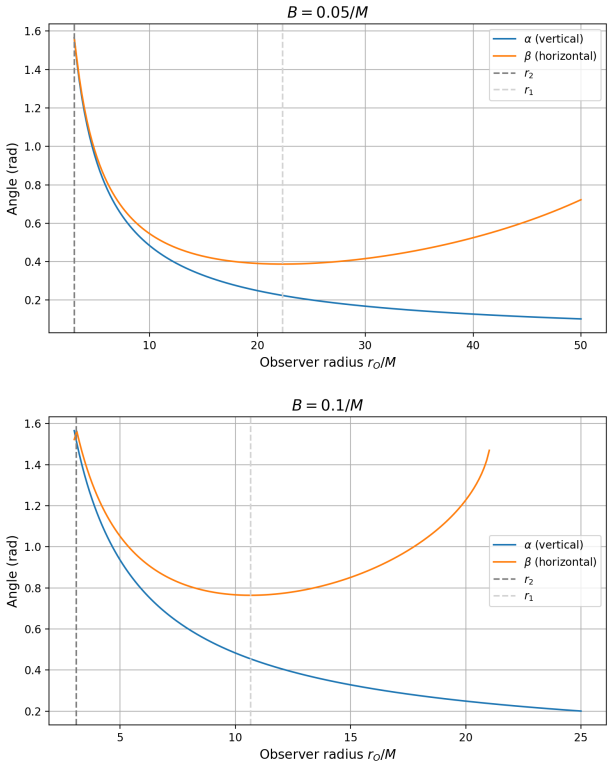

FIG. 5. Shadow vertical and horizontal angular radii vs. observer distance r_O in the equatorial plane.

For $r_S > r'_O$ (represented by the red vertical line in Fig. (6)) we define a critical value of the effective potential

$$V(r_S) = \left.\frac{E^2}{L^2}\right|_{crit}$$

corresponding to the point where the vertical line $r = r_S$ meets the plot of the potential. Hence, the light rays with $E^2/L^2 < E^2/L^2\big|_{crit}$ never reach r_S, so we associate darkness with these light rays, while light rays with $E^2/L^2 > E^2/L^2\big|_{crit}$ contribute to the bright regions. The borderline case, which gives the boundary of the shadow, is given by the outwardly directed light rays with $E^2/L^2\big|_{crit}$.

E. Horizontal Shadow Edge and Critical Distance

The horizontal angular radius β we derived corresponds to the largest equatorial angle from which a source can send a ray grazing r_2 to the observer. Solving $\sin^2\beta = 1$ gives us a critical observer radius r'_O beyond which no grazing ray reaches the observer. At exactly $r'_O = r_O(\beta = \pi/2)$ the entire horizontal diameter of the shadow subtends half the observer's sky, and for $r_O > r'_O$ no equatorial light ray with non-zero angular momentum can escape, consistent with Dhurandhar *et al.* [2]. The red dotted vertical line in Fig. (6) gives the critical radius

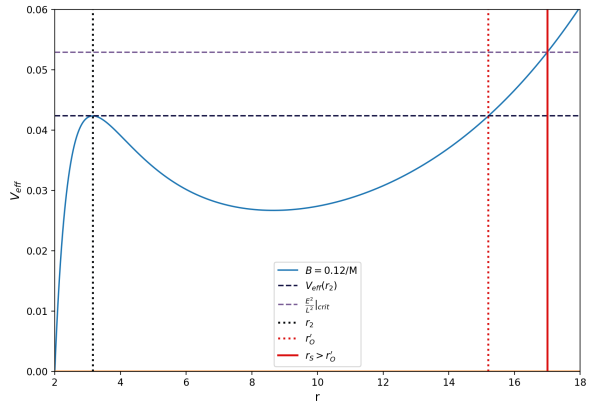

FIG. 6. Equatorial effective potential V_{eff} for $B = 0.12/M$.

r'_O for $B = 0.12/M$ which is plotted as a function of B in Fig. (7). For $B \to B_c$, where B_c is the critical magnetic field strength given by Eq. (7), $r'_O \to r_{1,2}$ and for $B \to 0$, $r'_O \to \infty$ as we recover the Schwarzschild case.

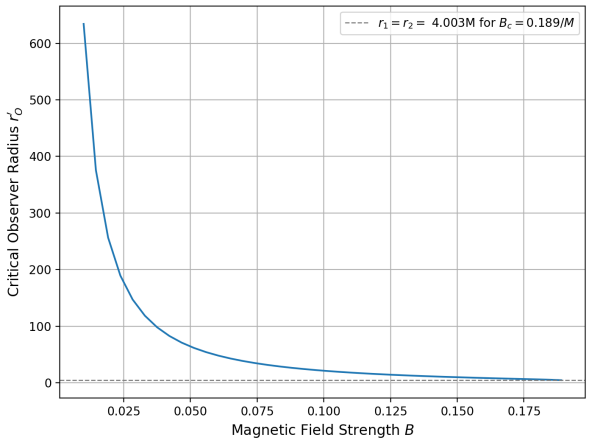

FIG. 7. Maximum observer radius r'_O vs magnetic field strength B.

The expression provides us with the value of $b_n = (L/E)_n$ that each light ray takes to form an image of order n for a polar observer.

VI. PHOTON RINGS IN ERNST SPACETIME

Photon rings correspond to geodesics looping multiple times around the black hole before reaching a distant observer. Aratore, Tsupko and Perlick [7] provide an expression for the impact parameter expressed in terms of the azimuthal shift for a spherically symmetric metric

$$b = b_{cr}\left[1 + F(r_s)F(r_O)\exp\left(-\frac{\Delta\tilde{\phi}}{\tilde{a}}\right)\right], \tag{29}$$

where

$$F(r_i) = \sqrt{\frac{2\beta_{ph}}{b_{cr}^2}}\left(1 - \frac{r_{ph}}{r_i}\right)\exp\left(\frac{k_i}{\tilde{a}}\right), \tag{30}$$

and $\Delta\tilde{\phi}$ is the shift of the total range of the angle $\tilde{\phi}$ swept out by a light ray that, starting at a light source at r_s, goes through a minimum radius and then arrives at an observer at r_O

$$\Delta\tilde{\phi} = (n+1)\pi - \cos^{-1}\left(\frac{\sin\varphi}{\sqrt{\sin^2\varphi + \cot^2\vartheta_O}}\right). \tag{31}$$

Here n corresponds to the number of half-turns the light ray makes around the black hole before reaching the observer and is termed as the *order of the image*. ϑ_O is the declination angle of the observer with respect to the axis of the black hole and φ is the polar angle formed on the observer's screen. See Fig. 1 in Tsupko [8] for illustrations. For a spacetime conformal to Schwarzschild, we have

$$r_{ph} = 3M, \tag{32}$$
$$b_{cr} = 3\sqrt{3}M, \tag{33}$$
$$\tilde{a} = 1, \tag{34}$$

$$k_i = \log\left(\frac{6}{3 - \eta_i + \sqrt{9 - 6\eta_i}}\right). \tag{35}$$

Inserting these values into the expression for b_n from Eq. (29) gets us, for a polar observer ($\theta_0 = \pi/2$)

$$b_n = 3\sqrt{3}M\left[1 + 216\left(1 - \frac{3M}{r_s}\right)\left(1 - \frac{3M}{r_O}\right)\frac{e^{-\left(n+\frac{1}{2}\right)\pi}}{\left(2 + \frac{3M}{r_s} + \sqrt{3 + \frac{18M}{r_s}}\right)\left(2 + \frac{3M}{r_O} + \sqrt{3 + \frac{18M}{r_O}}\right)}\right]. \tag{36}$$

A. Gap Parameter

Aratore, Tsupko and Perlick [7] defined the gap parameter as the relative separation between the radii of two consecutive photon rings normalized by the radius

of the bigger ring:

$$\Delta_n = \frac{b_n - b_{n+1}}{b_n}. \tag{37}$$

They have obtained a range of variability of the gap parameter for various spacetimes by changing the value of r_s from a chosen minimum value to infinity. The minimum radius in the case of Schwarzschild spacetime was chosen to be the Innermost Stable Circular Orbit (ISCO) given by $r_{ISCO} = 6M$ and the outer limit for r_s was chosen as infinity. We focus on the first non-trivial gap $\Delta_2 = (b_2 - b_3)/b_2$, which measures the separation between the $n = 2$ and $n = 3$ rings.

We showed in Sec. III D that stable timelike circular orbits can exist in the equatorial plane between the radii of the two circular lightlike geodesics. Thus, any circular timelike emitter must lie in

$$r_s \in (r_2, r_1).$$

B. Gap Parameter Intervals

For a given B value, we can evaluate the range of variability of the gap parameter for the Ernst spacetime for $r_s \in (r_{ISCO}, r_1)$. This is given by Figure (8). $B = 0$ is the Schwarzschild case and here $r_s \in (6M, \infty)$ for $r_O = \infty$ to match with the results obtained in Aratore, Tsupko and Perlick [7].

From Fig. (8) we can see that beyond a certain value of magnetic field strength B, the overlap between the range of gap parameter for the Schwarzschild-Melvin case and the Schwarzschild case is null. This corresponds to the case when $r_1 < 6M$ with $r = 6M$ being the ISCO for the Schwarzschild case. One determines this limit numerically to be $B = 0.160/M$. Thus, the gap parameter Δ_2 can help distinguish a Schwarzschild black hole from a Schwarzschild-Melvin black hole with the magnetic field strength $B = 0.160/M$.

VII. CONCLUSION

We investigated lightlike geodesics in the Schwarzschild–Melvin spacetime. Circular photon orbits exist in the equatorial plane for $B < B_c$, and meridional slices contain an unstable orbit at $r = 3M$. The vertical shadow radius remains unchanged from Schwarzschild, while the horizontal radius is increased by the magnetic field, producing an oblate shadow. We discussed the lensing effects in the equatorial plane for different observer and light source radii, and also obtained the angular deflection formula for the meridional plane. Using strong-deflection expansions, we computed the photon ring positions and their separations. These results provide an analytic basis for understanding shadow deformations due to magnetic fields.

Appendix A: Solutions of the Cubic Equation

The three roots of the cubic equation (6) are given by:

$$r_1 = \frac{(A+B)^{\frac{1}{3}}}{9B^2} - \frac{C}{9B^2\,(A+B)^{\frac{1}{3}}} + \frac{5M}{9} \tag{A1}$$

$$r_2 = \frac{-(1+i\sqrt{3})\,(A+B)^{\frac{1}{3}}}{18B^2} + \frac{(1-i\sqrt{3})C}{18B^2\,(A+B)^{\frac{1}{3}}} + \frac{5M}{9} \tag{A2}$$

$$r_3 = \frac{-(1-i\sqrt{3})\,(A+B)^{\frac{1}{3}}}{18B^2} + \frac{(1+i\sqrt{3})C}{18B^2\,(A+B)^{\frac{1}{3}}} + \frac{5M}{9} \tag{A3}$$

Where

$$A = 125B^6M^3 - 1188B^4M \tag{A4}$$

$$B = 18\sqrt{3}\sqrt{-375B^{10}M^4 + 1352B^8M^2 - 48B^6} \tag{A5}$$

$$C = -25B^4M^2 - 36B^2 \tag{A6}$$

[1] F. J. Ernst, Black holes in a magnetic universe, Journal of Mathematical Physics **17**, 54 (1976).

[2] S. V. Dhurandhar and D. N. Sharma, Null geodesics in the static Ernst space-time, Journal of Physics A: Mathematical and General **16**, 99 (1983).

[3] E. P. Esteban, Geodesics in the ernst metric, Il Nuovo Cimento B (1971-1996) **79**, 76 (1984).

[4] H. C. D. Lima Junior, P. V. P. Cunha, C. A. R. Herdeiro, and L. C. B. Crispino, Shadows and lensing of black holes immersed in strong magnetic fields, Physical Review D **106**, 044005 (2022).

[5] W. B. Bonnor, The magnetic curvature of space-time, Proceedings of the Physical Society, Section A **67**, 225 (1954).

[6] M. A. Melvin, Pure magnetic and electric geons, Physics Letters **8**, 65 (1964).

[7] F. Aratore, O. Y. Tsupko, and V. Perlick, Constraining spherically symmetric metrics by the gap between photon rings, Physical Review D **109**, 124057 (2024).

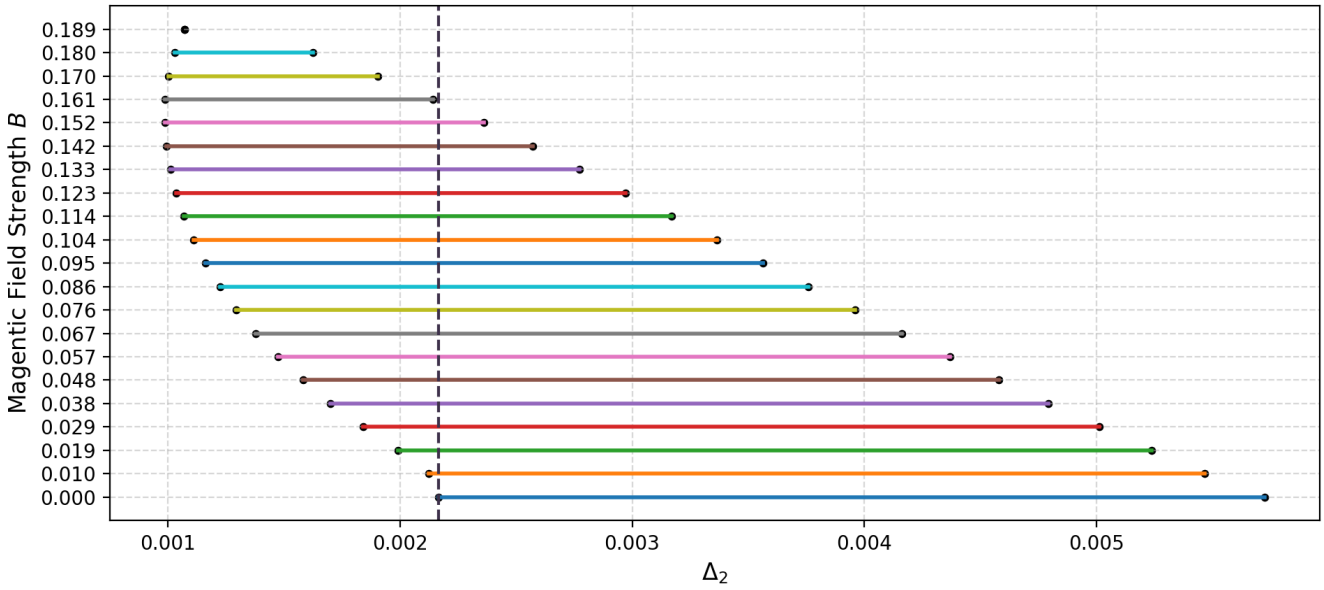

FIG. 8. Intervals of the gap parameter Δ_2, which is relative separation between $n = 2$ and $n = 3$ photon rings, for the different values of magnetic field strength B in Ernst spacetime. Each line segment shows Δ_2 as r_s varies from the innermost stable orbit up to r_1 (outer photon orbit). The last line is the Schwarzschild case ($B = 0$) while the top line is the critical case ($B_c = 0.189/M$). The vertical dashed line separates the Schwarzschild case from the Schwarzschild-Melvin cases with $B > 0.160/M$.

[8] O. Y. Tsupko, Shape of higher-order images of equatorial emission rings around a schwarzschild black hole: Analytical description with polar curves, Physical Review D **106**, 064033 (2022).